way. To confirm PA's specific involvement in the mTOR pathway, we used an S6K1 mutant ($\Delta N_{23}\Delta C_{104}$), the activity of which is resistant to rapamycin and sensitive to wortmannin (*27*). When transiently expressed in HEK293 cells, the rapamycin-resistant $\Delta N_{23}\Delta C_{104}$ mutant S6K1 activity was insensitive to butanol, whereas the recombinant wild-type S6K1 activity was inhibited by 1- and 2-butanol (Fig. 4A) to a similar extent as was the endogenous kinase (Fig. 2B). These observations support the hypothesis that PA signaling to S6K1 specifically goes through mTOR and not through PI3K . However, the specific PI3K inhibitor wortmannin abolished PA-stimulated S6K1 activation and 4E-BP1 phosphorylation (*26*), implying that PI3K is indispensable for the downstream response to PA. Based on the collective evidence, we propose a mechanism by which amino acid sufficiency sensed by the mTOR pathway, mitogenic stimulation of the mTOR pathway mediated by PA, and mitogenic stimulation of the PI3K pathway independent of PA are all required for full activation of S6K1 and 4E-BP1 (Fig. 4B). The observed PA stimulatory effect on these downstream effectors is likely dependent on the basal activity of PI3K in the absence of serum, which may also explain the fact that PA had a less potent stimulatory effect than did serum (Fig. 1).

Our findings reveal a mitogenic pathway upstream of S6K1 and 4E-BP1, which involves PA and probably its direct interaction with mTOR. The data suggest that rapamycin's inhibitory effect may derive from its competition with PA for binding to the FRB domain, preventing mTOR from activating downstream effectors but without inhibiting mTOR's catalytic activity. Another PIKK family member, DNA-PK, binds to inositol hexakisphosphate (IP_6), and its function in DNA double-strand break repair is regulated by IP_6 (*28*). The modulation of mTOR signaling by PA, together with DNA-PK stimulation by IP_6, may reveal a common theme of lipidlike molecules participating in regulation of PIKK proteins.

References and Notes

1. E. J. Brown *et al.*, *Nature* **369**, 756 (1994).
2. D. M. Sabatini, H. Erdjument-Bromage, M. Lui, P. Tempst, S. H. Snyder, *Cell* **78**, 35 (1994).
3. C. J. Sabers *et al.*, *J. Biol. Chem.* **270**, 815 (1995).
4. C. T. Keith, S. L. Schreiber, *Science* **270**, 50 (1995).
5. T. Schmelzle, M. N. Hall, *Cell* **103**, 253 (2000).
6. F. G. Kuruvilla, S. L. Schreiber, *Chem. Biol.* **6**, R129 (1999).
7. A. C. Gingras, B. Raught, N. Sonenberg, *Genes Dev.* **15**, 807 (2001).
8. A. C. Gingras, B. Raught, N. Sonenberg, *Annu. Rev. Biochem.* **68**, 913 (1999).
9. S. Fumagalli, G. Thomas, in *Translational Control of Gene Expression*, N. Sonenberg, J. W. B. Hershey, M. B. Mathews, Eds. (Cold Spring Harbor Laboratory Press, Cold Spring Harbor, NY, 2000), pp. 695–718.
10. E. J. Brown *et al.*, *Nature* **377**, 441 (1995).
11. G. J. Brunn *et al.*, *Science* **277**, 99 (1997).
12. P. E. Burnett, R. K. Barrow, N. A. Cohen, S. H. Snyder, D. M. Sabatini, *Proc. Natl. Acad. Sci. U.S.A.* **95**, 1432 (1998).
13. P. H. Scott, G. J. Brunn, A. D. Kohn, R. A. Roth, J. C. Lawrence Jr., *Proc. Natl. Acad. Sci. U.S.A.* **95**, 7772 (1998).
14. D. English, Y. Cui, R. A. Siddiqui, *Chem. Phys. Lipids* **80**, 117 (1996).
15. A. G. Buckland, D. C. Wilton, *Biochim. Biophys. Acta* **1483**, 199 (2000).
16. K. Fukami, T. Takenawa, *J. Biol. Chem.* **267**, 10988 (1992).
17. H. L. Reeves, M. G. Thompson, C. L. Dack, A. D. Burt, C. P. Day, *Hepatology* **31**, 95 (2000).
18. S. F. Yang, S. Freer, A. A. Benson, *J. Biol. Chem.* **242**, 477 (1967).
19. M. J. Cross *et al.*, *Curr. Biol.* **6**, 588 (1996).
20. M. Vilella-Bach, P. Nuzzi, Y. Fang, J. Chen, *J. Biol. Chem.* **274**, 4266 (1999).
21. J. Chen, X. F. Zheng, E. J. Brown, S. L. Schreiber, *Proc. Natl. Acad. Sci. U.S.A.* **92**, 4947 (1995).
22. J. Choi, J. Chen, S. L. Schreiber, J. Clardy, *Science* **273**, 239 (1996).
23. J. P. Segrest *et al.*, *J. Lipid Res.* **33**, 141 (1992).
24. Y. Barenholz *et al.*, *Biochemistry* **16**, 2806 (1977).
25. Y. Fang, M. Vilella-Bach, J. Chen, unpublished data.
26. Supplementary Web material is available on *Science* Online at www.sciencemag.org/cgi/content/full/294/5548/1942/DC1.
27. Q. P. Weng, K. Andrabi, M. T. Kozlowski, J. R. Grove, J. Avruch, *Mol. Cell. Biol.* **15**, 2333 (1995).
28. L. A. Hanakahi, M. Bartlet-Jones, C. Chappell, D. Pappin, S. C. West, *Cell* **102**, 721 (2000).
29. J. E. Kim, J. Chen, *Proc. Natl. Acad. Sci. U.S.A.* **97**, 14340 (2000).
30. HEK293 cells were maintained in Dulbecco's modified Eagle medium (DMEM) containing 10% fetal bovine serum (FBS) at 37°C with 5% CO_2. Serum starvation of cells was carried out in serum-free DMEM for 24 hours. For amino acid deprivation, the cells were incubated in Dulbecco's phosphate-buffered solution containing 10% dialyzed FBS for 2 hours. Transient transfections were performed with SuperFect or PolyFect (Qiagen, Valencia, CA). The amount of plasmid DNA transfected per well in six-well plates was 1 μg of mTOR, 1 μg of S6K1, and 0.4 μg of 4E-BP1.
31. All bacterial expression plasmids were constructed in pGEX-2T (Pharmacia), and all mammalian expression plasmids were constructed in pCDNA3 (Invitrogen). pCDNA-FLAG-mTOR/S2035T, pCDNA-FLAG-mTOR/S2035T/D2357E (kinase-dead), pCDNA-Myc-S6K1 (p70s6k), pCDNA-FLAG-4E-BP1, pGEX-FRB (wild type), and pGEX-FRB/S2035I were previously described (*20*, *29*). $\Delta N_{23}\Delta C_{104}$ S6K1 (amino acids 24 to 398) cDNA was amplified by polymerase chain reaction (PCR) and inserted into pCDNA-Myc via Not I and Xba I sites. All point mutations were generated by nested PCR using Bam HI and Eco RI as the flanking sites for pGEX-FRB constructs and Kpn I and Hpa I for pCDNA-FLAG-mTOR constructs. Glutathione *S*-transferase (GST)–FKBP12 and various FRB proteins were expressed and purified from *Escherichia coli* strain BL21, as described previously (*20*).

32. We thank J. George for technical guidance with the lipid binding assays, J. Clardy for suggestions regarding the FRB structure, and Z. Liu for discussions about the manuscript. Supported by NIH R01 grant GM58064 and American Heart Association Midwest Affiliate grant 9951123Z.

5 September 2001; accepted 23 October 2001

Regulation of Cell Survival by Secreted Proneurotrophins

Ramee Lee, Pouneh Kermani, Kenneth K. Teng, Barbara L. Hempstead*

Neurotrophins are growth factors that promote cell survival, differentiation, and cell death. They are synthesized as proforms that can be cleaved intracellularly to release mature, secreted ligands. Although proneurotrophins have been considered inactive precursors, we show here that the proforms of nerve growth factor (NGF) and the proforms of brain derived neurotrophic factor (BDNF) are secreted and cleaved extracellularly by the serine protease plasmin and by selective matrix metalloproteinases (MMPs). ProNGF is a high-affinity ligand for $p75^{NTR}$ with high affinity and induced $p75^{NTR}$-dependent apoptosis in cultured neurons with minimal activation of TrkA-mediated differentiation or survival. The biological action of neurotrophins is thus regulated by proteolytic cleavage, with proforms preferentially activating $p75^{NTR}$ to mediate apoptosis and mature forms activating Trk receptors to promote survival.

The neurotrophin family of growth factors, including NGF, BDNF, and neurotrophins-3 and -4 (NT-3, NT-4) regulates neuronal survival and synaptic plasticity (*1*). They are synthesized as precursors (proneurotrophins) that are proteolytically cleaved to mature, biologically active neurotrophins (*2*). Because neurotrophins are normally expressed at low levels, little is known about their processing and secretion by neurons and non-neuronal cells in vivo. However, when expressed in heterologous cells, proneurotrophins are secreted as well as cleaved intracellularly by furin or proconvertases at a highly conserved dibasic amino acid cleavage site for secretion as stable, noncovalent dimers (*3*, *4*). Mature neurotrophins selectively bind to members of the Trk family of receptor tyrosine kinases, but they also interact with low affinity to a structurally distinct receptor, $p75^{NTR}$. Although $p75^{NTR}$ can increase the affinity and specificity of Trk-neurotrophin

Division of Hematology, Department of Medicine, Weill Medical College of Cornell University, 1300 York Avenue, New York, NY 10021, USA.

*To whom correspondence should be addressed: E-mail: blhempst@med.cornell.edu

interactions, $p75^{NTR}$ can also induce apoptosis in oligodendrocytes, neurons, and vascular smooth muscle cells when Trk activation is reduced or absent (*5*). High doses of neurotrophin elicit cell death through $p75^{NTR}$, indicating that $p75^{NTR}$ signaling is relatively limited in comparison to that of other receptors of the tumor necrosis factor (TNF) receptor superfamily (*5*).

Defined functions for the neurotrophin prodomains have been limited to promoting the folding of the mature domain (*6–8*) and to sorting neurotrophins to either constitutive or regulated secretory pathways (*9*). However, sequence comparison of proneurotrophins revealed regions of the prodomain that are highly conserved across species, suggesting that they may mediate additional biological actions (*10*). To assess this possibility, the expression of proNGF and proBDNF in adult mouse tissues was determined (*11*). Using antibodies specific for the mature domains of NGF or BDNF (*11*), immunoreactive proteins with molecular masses of 18 to 30 kD were detected, in addition to the 13.5-kD mature forms of NGF and BDNF (*11*, *12*). This suggested that tissue-specific proteolytic processing of proneurotrophins occurs in vivo.

Because proneurotrophins are secreted by cells (*4*, *11*, *12*) and contain consensus sites for cleavage by plasmin and by MMP-3 and MMP-7 (*13*), we considered whether secreted proneurotrophins could be cleaved extracellularly by such proteases. Both plasmin and MMPs exhibit expression patterns consistent with neurotrophin action: at the synapse, where mature BDNF can activate presynaptic and postsynaptic TrkB receptors (*14*), and on endothelial cell surfaces, where mature BDNF promotes TrkB-mediated endothelial cell survival (*15*).

BDNF was harvested from the media of 293 or endothelial cells that were infected with recombinant adenovirus encoding BDNF (*16*). In addition to 13.5-kD mature BDNF, proBDNF forms of molecular mass 30, 28, and 24 kD, and those of mass 28 kD, were detected by a BDNF-specific antibody in the media of 293 cells and endothelial cells, respectively (Fig. 1, A and B). Addition of plasmin, MMP-3, or MMP-7 to the harvested media reduced the amount of the 30-kD proBDNF (Fig. 1A). The 28-kD proBDNF from endothelial cell media was also cleaved by plasmin and MMP-7 but not MMP-3, possibly reflecting differences in expression of tissue inhibitors of metalloproteinases by endothelial and 293 cells (Fig. 1B). MMP-7 treatment of secreted proBDNF from 293 or endothelial cells yielded a 17-kD proBDNF form, suggesting that cleavage occurred approximately 90 amino acids from the NH_2-terminus (*11*). Incubation of plasmin or MMP-7 with specific inhibitors verified the specificity of these proteolytic events.

To confirm the extracellular cleavage of proBDNF, endothelial cells expressing BDNF were incubated with plasmin before media collection (Fig. 1C). Inhibition of plasmin activity by the cell-impermeable inhibitor aprotinin reduced cleavage of proBDNF, suggesting that these higher molecular weight forms are released from cells and then cleaved by plasmin at the cell surface. Thus, in addition to furin, cleavage of proneurotrophins can be regulated selectively by plasmin and MMPs.

To analyze the cleavage of secreted proNGF, a point mutation in the dibasic site used by furin was generated to impair intracellular proteolysis (*17*). Furin-resistant proNGF was expressed in 293 cells (Fig. 1D), and, when secreted, was cleaved by plasmin to a 13-kD form (Fig. 1E). In addition, incubation with MMP-7 but not MMP-2, -3, or -9 resulted in cleavage of the 30-kD proNGF to the 17-kD form (Fig. 1E).

To evaluate whether proneurotrophins selectively bind and activate Trk and $p75^{NTR}$ receptors, furin-resistant proNGF and mature NGF were purified from the media of transfected 293 cells (Fig. 1D), and their ability to bind TrkA or $p75^{NTR}$ was determined (Fig. 2) (*18*). Cells expressing either TrkA or $p75^{NTR}$ were treated with radiolabeled mature NGF and either unlabeled proNGF or unlabeled mature NGF. Unlabeled mature NGF displaced binding of radiolabeled mature NGF from TrkA expressing cells with an IC_{50} (concentration of inhibitor that reduced binding by 50%) of 1.2 nM, in agreement with equilibrium binding studies [dissociation constant (K_d) = 1 nM] (*19*, *20*). However, furin-resistant proNGF was ineffective in displacing mature NGF bound to TrkA, with an IC_{50} of greater than 5 nM. Mature NGF also

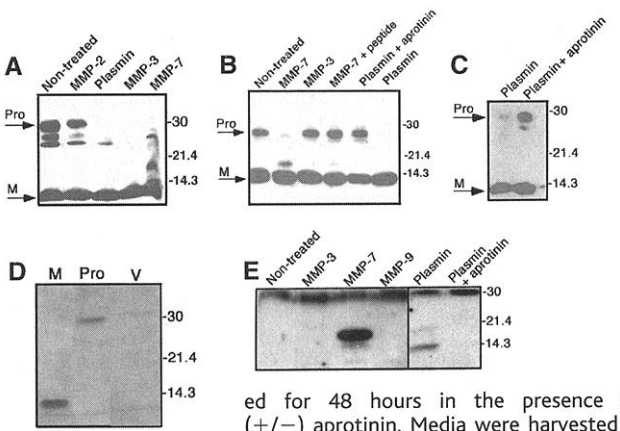

Fig. 1. Cleavage of secreted proBDNF and proNGF by candidate proteinases. Harvested media of BDNF-expressing 293 cells (**A**), or murine endothelial cells (**B**) was incubated with the indicated proteinases, and cleavage products were probed in Western blot analysis with antibody to BDNF (*16*). To confirm enzymatic specificity, plasmin was incubated with the inhibitor aprotinin or MMPs were incubated with a peptide inhibitor. (**C**) Endothelial cells expressing BDNF were incubated for 48 hours in the presence of plasmin with or without (+/−) aprotinin. Media were harvested and analyzed by Western blot. (**D**) Purification of mature NGF (M) and cleavage-resistant proNGF (Pro) from media from 293 cells stably expressing native NGF, of a furin-resistant form of NGF with a His tag at the COOH-terminus, or of the vector alone (V) with the use of Ni-column chromatography (*17*). Proteins eluted with imidazole were analyzed by SDS–polyacrylamide gel electrophoresis (SDS-PAGE) and silver staining. (**E**) Purified furin-resistant proNGF was incubated with the indicated proteinases with or without (+/−) inhibitors and proteolytic products were detected by Western blot analysis with antibody to NGF. The inability of MMP-3 to cleave proNGF, as compared to proBDNF, may reflect sequence differences at the putative MMP site.

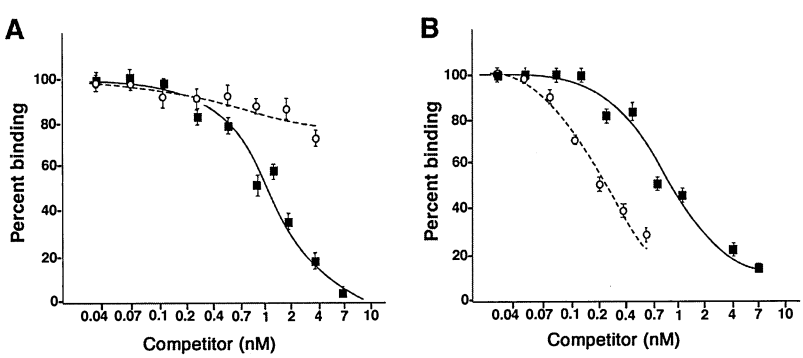

Fig. 2. Binding analysis of mature and cleavage-resistant proNGF to TrkA or $p75^{NTR}$ receptors. Dilutions of purified furin-resistant proNGF (Fig. 1D), or commercial mature NGF were assayed for their ability to displace ^{125}I-radiolabeled commercial mature NGF (1 nM) from 293 cells expressing TrkA (**A**) or from A875 cells expressing $p75^{NTR}$ (**B**) (*28*). Squares, commercial mature NGF; open circles, cleavage resistant proNGF. Competition with purified mature NGF yielded results that were comparable to those obtained with commercial NGF (*18*).

displaced radiolabeled mature NGF bound to $p75^{NTR}$ with an IC_{50} of 1.0 nM, consistent with equilibrium binding studies (K_d = 1.3 nM) (*19*). However, furin-resistant proNGF bound to $p75^{NTR}$ with five times greater affinity than mature NGF, with an IC_{50} of 0.2 nM. These results demonstrate that proNGF is the preferred ligand for $p75^{NTR}$ but not TrkA, and they suggest that $p75^{NTR}$-dependent cellular processes might be more efficiently induced by proNGF than by mature NGF.

To determine whether the higher affinity binding of proNGF to $p75^{NTR}$ resulted in enhanced $p75^{NTR}$-mediated apoptosis, we used a vascular smooth muscle cell line expressing $p75^{NTR}$ but not Trk receptors, which exhibits dose-dependent apoptosis upon addition of NGF (*21*). Cells were exposed to purified mature NGF or furin-resistant proNGF (*22*). Treatment of cells with mature NGF from commercial sources (predominantly mature NGF) induced apoptosis in 20% of the cells at 2 nM concentration (~50 ng/ml) (*5*, *21*) (Fig. 3A). In contrast, treatment of cells with proNGF was at least 10 times more potent than mature NGF in inducing apoptosis in 18% of cells at 0.1 nM. This result, together with the binding data (Fig. 2B), suggests that occupancy of less than 30% of $p75^{NTR}$ receptors with furin-resistant proNGF can induce apoptosis.

To determine the relative activities of mature NGF and furin-resistant proNGF in activating Trk-mediated cellular responses, we assessed TrkA autophosphorylation in dose-response studies (*22*) (Fig. 3B). Mature NGF and commercial NGF induced TrkA autophosphorylation at a concentration of 0.2 nM. However, furin-resistant proNGF did not induce TrkA phosphorylation even at concentrations of 1 nM, consistent with the observed reduction in TrkA binding (Fig. 2A). To assess the functional consequences of proNGF-TrkA interactions, TrkA-expressing PC12 cells and dissociated superior cervical ganglia (SCG) neurons were used in neurite outgrowth assays (Fig. 3, C and D). Treatment of PC12 cells with purified mature NGF or commercial NGF induced neurite elongation at 0.2 to 0.4 nM concentration. However, reduced neurite outgrowth was observed in PC12 cells or SCG neurons that were treated with the furin-resistant proNGF at concentrations of 0.2 to 0.8 nM, consistent with prior reports that proneurotrophins are less active than the mature forms in promoting Trk-mediated neuronal survival (*6*) and in activating Trk receptors (*3*). Treatment of SCG neurons, which coexpress both $p75^{NTR}$ and TrkA (*23*), with proNGF resulted in cell death (Fig. 3D). Taken together, these results suggest that the cleavage-resistant proform of NGF is a high-affinity, functional ligand for the pro-apoptotic $p75^{NTR}$ receptor, whereas the proteolytically cleaved mature NGF is the preferred ligand for TrkA.

These studies shed light on the often-conflicting roles for $p75^{NTR}$ in mediating apoptosis (*23–25*) and in augmenting Trk-induced survival and differentiation (*5*). The selectivity of proNGF for $p75^{NTR}$ suggests that its local secretion may determine whether apoptotic or survival actions predominate. Thus, despite widespread $p75^{NTR}$ expression, an evaluation of proneurotrophin expression should clarify the spatial and temporal restriction of apoptosis in injured neuronal tissues (after seizures, inflammation, or degeneration) and in injured blood vessels where neurotrophins, $p75^{NTR}$, and Trk receptors are coexpressed (*1*, *26*). The regulated activity of proteases such as plasmin and selective MMPs may further define these proapoptotic or prosurvival effects of neurotrophins. Examination of potential biological activities for the precursor forms of other growth factors, such as glial derived neurotrophic factor and neuregulins, whose cleaved forms bind to multicomponent receptors, may uncover differential activation of individual receptor components.

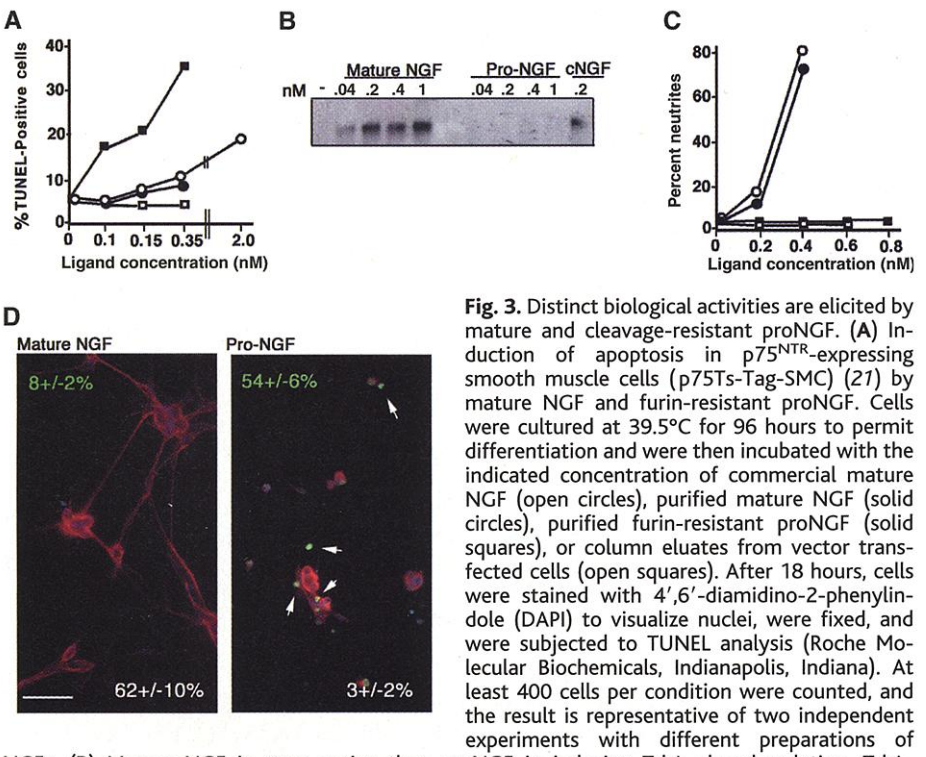

Fig. 3. Distinct biological activities are elicited by mature and cleavage-resistant proNGF. (**A**) Induction of apoptosis in $p75^{NTR}$-expressing smooth muscle cells (p75Ts-Tag-SMC) (*21*) by mature NGF and furin-resistant proNGF. Cells were cultured at 39.5°C for 96 hours to permit differentiation and were then incubated with the indicated concentration of commercial mature NGF (open circles), purified mature NGF (solid circles), purified furin-resistant proNGF (solid squares), or column eluates from vector transfected cells (open squares). After 18 hours, cells were stained with 4′,6′-diamidino-2-phenylindole (DAPI) to visualize nuclei, were fixed, and were subjected to TUNEL analysis (Roche Molecular Biochemicals, Indianapolis, Indiana). At least 400 cells per condition were counted, and the result is representative of two independent experiments with different preparations of NGFs. (**B**) Mature NGF is more active than proNGF in inducing TrkA phosphorylation. TrkA-expressing 293 cells were cultured in reduced serum for 18 hours, followed by either the addition of diluent (–) or of mature NGF, proNGF, or commercial NGF (cNGF) at the indicated concentrations for 10 min. Immunoprecipitations using antibody to Trk were analyzed by Western blot with antibody to phosphotyrosine. (**C** and **D**) Effects of mature and cleavage resistant proNGF on neuritogenesis using PC12 cells (C) or SCG neurons (D). Cells were treated with mature NGF (solid circles), cleavage-resistant proNGF (solid squares), or commerical mature NGF (open circles) at the indicated concentration or with the control column eluates from vector-transfected cells (open squares) for 48 hours in serum-free media, and cells were evaluated for neurite processes greater than one cell body in length. SCG neurons were treated with 0.4 nM mature or proNGF for 36 hours and were fixed. Trk was detected using rhodamine-conjugated antibody to Trk, TUNEL analysis performed with fluorescein isothiocyanate–deoxyuridine 5′-triphosphate (FITC-dUTP), and nuclei were detected by DAPI staining. The percentage of neurite-expressing cells (white typeface) and apoptotic cells (green typeface) is indicated. Cells treated with diluent alone yielded 30 ± 10% apoptosis. Scale bar, 30 μm. At least 200 cells per condition were scored, and results are representative of three independent experiments using different preparations of NGFs.

References and Notes

1. A. Patapoutian, L. F. Reichardt, *Curr. Opin. Neurobiol.* **11**, 272 (2001).
2. R. H. Edwards, M. J. Selby, P. D. Garcia, W. J. Rutter, *J. Biol. Chem.* **263**, 6810 (1988).
3. S. J. Mowla *et al.*, *J. Biol. Chem.* **276**, 12660 (2001).
4. J. V. Heymach, E. M. Shooter, *J. Biol. Chem.* **270**, 12297 (1995).
5. F. S. Lee, A. H. Kim, G. Khursigara, M. V. Chao, *Curr. Opin. Neurobiol.* **11**, 281 (2001).
6. U. Suter, J. V. Heymach, E. M. Shooter, *EMBO J.* **10**, 2395 (1991).
7. A. Rattenholl *et al.*, *J. Mol. Biol.* **305**, 523 (2001).
8. R. Kolbeck, S. Jungbluth, Y.-A. Barde, *Eur. J. Biochem.* **225**, 995 (1994).
9. H. W. Farhadi *et al.*, *J. Neurosci.* **20**, 4059 (2000).
10. G. Heinrich, T. Lum, *Int. J. Dev. Neurosci.* **18**, 1 (2000).
11. Web figure 1 is available at *Science* Online at www.sciencemag.org/cgi/content/full/294/5548/1945/DC1.
12. M. Fahnestock *et al.*, *Mol. Cell. Neurosci.* **18**, 210 (2001).

13. M. M. Smith, L. Shi, M. Navre, *J. Biol. Chem.* **270**, 6440 (1995).
14. M. M. Poo, *Nature Rev. Neurosci.* **2**, 24 (2001).
15. M. Donovan *et al.*, *Development* **127**, 4531 (2000).
16. Recombinant adenovirus encoding rat BDNF (*27*) was used to infect 293 cells or a temperature-sensitive SV40 T antigen transformed murine cardiac microvascular endothelial cell line at a multiplicity of infection of 100 or 200, respectively. Forty-eight-hours after infection, BDNF in the media was harvested and incubated with plasmin (3 μg/ml; American Diagnostics, Greenwich, CT) with or without (+/−) aprotinin (3 μl/ml; Sigma, St. Louis, MO), MMP-2, -3, -7 (10 μl/ml; Calbiochem, San Diego, CA) or harvested and incubated with MMP-9 (10 μl/ml; Oncogene, Cambridge, MA) with or without (+/−) MMP inhibitor (5 μl/ml, Calbiochem) for 1 hour at 37°C. Purified proNGF (0.8 μg/ml) (*17*) was used for proteolytic digestion in parallel samples. Cleavage products were detected by Western blot analysis using antibody specific for mature BDNF or mature NGF.
17. The cDNA encoding mouse NGF was amplified by reverse transcriptase–polymerase chain reaction (RT-PCR) and was bidirectionally sequenced. To improve translation initiation, 11 bases from mouse 5′ untranslated region (UTR) of mouse NT-3 including the Kozak consensus were exchanged for the mouse NGF sequence [GenBank M35075, base pairs (bp) 84 to 95] immediately 5′ of the initiating methionine. Using PCR-based mutagenesis, six histidine (His) residues were added at the COOH-terminus, and residues RR (bp 1008 to 1013) near the COOH-terminus were mutated to AA to prevent cleavage of the His-tag. To generate proNGF with impaired furin-cleavage, residues RR (bp 531 to 536) were mutated to AA using PCR. After bidirectional sequencing, constructs were subcloned into the expression vector pCDNA and stably transfected 293 cells were isolated after selection in G418 containing medium. Cells were incubated in serum-depleted media for 18 hours, and the media was collected and depleted of cells by centrifugation. His-tagged mature or furin-resistant proNGF was purified using Ni-bead chromatography (Xpress System Protein Purification; Invitrogen, Carlsbad, CA) per manufacturer's methods with the use of 350 mM imidazole for elution. Medium from 293 cells stably transfected with vector alone was harvested in parallel.
18. Mouse NGF (Harlan, Indianapolis, IN) was radioiodinated using lactoperoxidase and hydrogen peroxide as described (*28*) to an average specific activity of 3000 disintegrations per minute (dpm)/fmol and was used within 2 weeks. Competition analysis of equilibrium binding was performed using a whole-cell assay. A875 melanoma cells expressing $p75^{NTR}$ but not Trk receptors or 293 cells stably transfected with pCDNA-rat TrkA (*17*) were resuspended at 0.75 × 10^6 cells/ml final concentration. Cells were incubated with 1 nM radioiodinated NGF in the presence or absence of unlabeled mature NGF or unlabeled proNGF from 0.005 to 7 nM concentration and binding proceeded for 1 hour at 0.4°C. Cell-bound NGF was separated from free NGF by centrifuging through calf serum. Each condition was assessed in quadruplicate. Nonspecific binding measured in parallel incubation with 500-fold excess mature NGF was less than 10% of total binding. Results corrected for this nonspecific binding were expressed as the mean ± standard deviation. The PRISM program was used to generate the IC_{50} with the use of linear regression.
19. B. L. Hempstead *et al.*, *Nature* **350**, 678 (1991).
20. A. Schropel, D. von Schack, G. Dechant, Y. A. Barde, *Mol. Cell. Neurosci.* **6**, 544 (1995).
21. S. Wang *et al.*, *Am. J. Pathol.* **157**, 1247 (2000).
22. 293 cells expressing TrkA were serum-starved for 18 hours and then neurotrophins were added for 10 min before cell harvest. TrkA was immunoprecipitated with pan-Trk antibody (*19*), and Western blots probed with antibody to phosphotyrosine. TrkA-expressing PC12 cells (*29*) were used for neuritogenesis assays, and freshly isolated SCG from P0 rat pups were used on collagen substrate.
23. S. X. Bamji *et al. J. Cell Biol.* **140**, 911 (1998).
24. J. M. Frade, A. Rodriguez-Tebar, Y.-A. Barde, *Nature* **383**, 166 (1996).
25. P. Cassacia-Bonnefils, B. D. Carter, R. T. Dobrowski, M. V. Chao, *Nature* **383**, 716 (1996).
26. M. J. Donovan *et al.*, *Am. J. Pathol.* **147**, 309 (1995)
27. E. Benraiss *et al.*, *J. Neurosci.* **21**, 6718 (2001).
28. D. Mahadeo *et al.*, *J. Biol. Chem.* **269**, 6884 (1994).
29. B. L. Hempstead *et al.*, *Neuron* **9**, 883 (1992).
30. Supported by NIH grant NS30687, the Burroughs Wellcome Fund and the American Heart Association (to B.L.H.), and NIH grant T32 EY07138. We thank M. Chao, J. Salzer, D. Falcone, I. Feit, K. Hajjar, and S. Rafii for comments; C. Cummins and M. Kobi for technical assistance; and C. Wieland for manuscript preparation. Adenoviral vectors were kindly provided by S. Goldman, and murine endothelial cells were provided by B. Weksler and D. Poulan.

3 August 2001; accepted 25 October 2001

Lobster Sniffing: Antennule Design and Hydrodynamic Filtering of Information in an Odor Plume

M. A. R. Koehl,[1]* Jeffrey R. Koseff,[2] John P. Crimaldi,[2]† Michael G. McCay,[1] Tim Cooper,[1] Megan B. Wiley,[2] Paul A. Moore[3]

The first step in processing olfactory information, before neural filtering, is the physical capture of odor molecules from the surrounding fluid. Many animals capture odors from turbulent water currents or wind using antennae that bear chemosensory hairs. We used planar laser–induced fluorescence to reveal how lobster olfactory antennules hydrodynamically alter the spatiotemporal patterns of concentration in turbulent odor plumes. As antennules flick, water penetrates their chemosensory hair array during the fast downstroke, carrying fine-scale patterns of concentration into the receptor area. This spatial pattern, blurred by flow along the antennule during the downstroke, is retained during the slower return stroke and is not shed until the next flick.

Many animals use chemical cues in the water or air around them to detect mates, competitors, food, predators, and suitable habitats (*1–3*). Large-scale turbulent flow in the environment carries odorants from a source to an animal's olfactory organ (such as an antenna or nose), while small-scale laminar flow near the organ's surface and molecular diffusion transport odorants to the receptors (*2*, *4*). Turbulent fluid motion on a scale of meters to millimeters (*5*) determines the patchy intermittent structure of odor plumes in the environment (*6*); hence, chemical signals monitored at a point downstream from an odor source fluctuate in terrestrial (*7*, *8*) and aquatic (*9*, *10*) habitats and in laboratory flumes (*11–12*). Recent attention has focused on the relation between the neural output of antennae and of the brain antennal lobe of moths in odor plumes (*13*) and on the neural processing of odorant pulses (*14*). We used lateral antennules of spiny lobsters, *Panulirus argus*, to analyze the critical first step in determining the spatial and temporal patterns of odor pulses arriving at receptors: the physical interaction of the olfactory organ with an odor plume. *P. argus* lateral antennules (Fig. 1A) bear rows of aesthetascs (hairs containing hundreds of chemoreceptor cells) flanked by larger guard hairs (*15*) and thus provide a system for investigating the design of hair-bearing olfactory antennae (*16*, *17*).

Fluid flow around a hair in an array depends on the relative importance of inertial and viscous forces, as represented by the Reynolds number (Re) (*18*). Because the fluid in contact with the surface of a moving object does not slip relative to the object, a velocity gradient develops in the flow around the object. The smaller or slower the object (that is, the lower its Re), the thicker this boundary layer of sheared fluid is relative to the size of the object. If the boundary layers around the hairs in an array are thick relative to the gaps between hairs, then little fluid leaks through the array. Hair arrays undergo a transition between nonleaky paddlelike behavior and leaky sievelike behavior as Re is increased (*19–21*). Although flow velocity has only a small effect on the rate of molecule

[1]Department of Integrative Biology, University of California, Berkeley, CA 94720–3140, USA. [2]Environmental Fluid Mechanics Laboratory, Department of Civil and Environmental Engineering, Stanford University, Stanford, CA 94305–4020, USA. [3]Department of Biological Sciences and the J. P. Scott Center for Neuroscience, Mind, and Behavior, Bowling Green State University, Bowling Green, OH 43403, USA.

*To whom correspondence should be addressed. E-mail: cnidaria@socrates.berkeley.edu

†Present address: Department of Civil, Environmental, and Architectural Engineering, University of Colorado, Boulder, CO 80309–0428, USA.